Indoor 3-D Localization over LCX-based Wireless Environment Using Particle Filter Approach

Junjie Zhu, Kenta Nagayama, Erika Kouda, Yafei Hou, Satoshi Denno
Graduate School of Natural Science and Technology, Okayama University, Okayama, Japan
Contact author: Yafei Hou, yfhou@okayama-u.ac.jp

***Abstract*—Localization, as a key technology, has promoted various location-based services and applications. It also plays an important role in many novel systems such as the Internet of Things (IoT), smart buildings and houses, and unmanned aerial vehicle (UAV) systems. Different from the requirements for localization technology in the past, today's indoor localization systems need to provide not only the two-dimensional (2-D) location information of the target but also stable three-dimensional (3-D) information. Most of the existing localization methods in wireless communication consider the communication systems using conventional monopole antennas. However, in many application scenarios such as smart manufacturing factories, the shielding and interference effects of metallic objects on radio waves limit the performance of conventional monopole antennas. It is often necessary to increase the number of access points (APs) with additional complexity and cost to guarantee entire wireless coverage. Leaky coaxial cable (LCX) which can be used as antennas for wireless communication can be employed to solve this problem. As a long and flexible cable, LCX can provide promising wireless coverage for stable wireless communication and localization. This paper proposes a 3-D localization method using multiple LCXs in an indoor environment. The proposal is based on a particle filter algorithm and uses the time of arrival (TOA) of the signal as the indicator for filtering.**

***Index Terms*—Leaky Coaxial Cable (LCX), indoor localization, particle filter, unmanned aerial vehicles**

I. Introduction

With the rapid growth of portable devices and Internet of Things (IoT) devices in the 5G era, location-awareness has become a key and basic technical support for many novel application scenarios and systems such as autonomous vehicles [1], smart houses and buildings [2] and IoT systems [3]. These application scenarios are usually considered in indoor propagation environments where the Global Position System (GPS) signal is weak or even not available. Therefore, the capability of powerful and reliable two-dimensional (2-D) or three-dimensional (3-D) localization has become a necessity.

Unmanned aerial vehicle (UAV) is a recent technology that can be employed in various indoor applications such as automated factories and smart logistics warehouses [4]. Different from robots working on the ground, UAVs act based on 3-D location information. As the key to this application scenario, the 3-D localization for UAVs can assist the flight of the UAVs and improve the wireless communication quality between the UAVs and the base stations by using the beamforming technology based on location information [5].

Due to the problem of the non-line-of-sight (NLOS) signal propagation in the indoor environment and the noise in the signal measurement process, range-based localization methods, which map the characteristic information of the signal (such as angle of arrival (AOA), received signal strength indicator (RSSI), time of arrival (TOA), and time difference of arrival (TDOA)) to range values and then derive the location of the target using multilateration methods, do not have reliable localization performance. Machine learning (ML) algorithms are employed to improve localization performance in recent research [6], [7]. ML methods such as fingerprinting-based systems usually act as an enhanced classifier and it consists of two phases including an off-line phase and an on-line phase. In the off-line phase, the signal information with location labels is measured as the data set for training. The trained model is used to classify the signal data, whose locations are unknown, into different location classes in the on-line phase. In addition to ML, methods involving extended Kalman filter and particle filter have been proposed for achieving better localization accuracy. In particular, the particle filter algorithm has high expectations due to its promising performance in the solution of the associated nonlinearities and the intractable computation of the probability distributions [8]. Compared with other conventional methods, localization and tracking methods based on the particle filter can estimate the state of the dynamic system from the noisy or incomplete observation sequence and have better performance in noisy environments [9], [20].

Most localization processes usually consider the wireless communication system using conventional monopole antennas for signal transmission and reception. These localization schemes rely on the target's radio signal being effectively received by multiple access points (APs) nearby. However, application scenarios including automated factories and smart logistics warehouses are usually full of large machinery and equipment which can be seen as metal barriers. Due to the shielding and influence of the radio waves by metal objects, some areas in the smart factory environment are similar to the radio quiet zone (RQZ) where wireless signals cannot be sent and received normally. When the target passes or stays in these areas, the system can not perform wireless communication and localization. It is often necessary to increase the number of APs with additional complexity and cost to guarantee entire wireless coverage. This problem can be solved by using the leaky coaxial cable (LCX) for wireless communication and localization. LCX can be used as antennas for wireless communication and has many potential advantages

978-1-6654-9122-8/23/$31.00

due to its unique characteristics. As a long and flexible cable, LCX can bypass various metal obstacles to adapt to various irregular spaces and has a simple installation process. References [10] and [11] show the uniform wireless coverage of LCX and the low interference between cells. In [12], it shows the employment of LCX in train and the train ground communication system. The research on using LCX to provide wireless power transfer for moving objects is shown in [13]. LCX can also be used for multi-input multi-output (MIMO) communication, and the authors propose a 2-by-2 LCX-MIMO system using the bi-directional radiation property of LCX [14]. To improve the channel capacity, an effective 4-by-4 LCX-MIMO system and a simple power allocation method using the user's location information are proposed in [15]. On the other hand, localization using LCX has been researched for a few years. 2-D Indoor localization methods based on TOA, TDOA, and RSSI are proposed in [16]-[18] respectively.

The motivation of this paper is to propose a particle filter-based localization method for 3-D location awareness in the indoor environment. This localization system uses multiple LCXs as the APs to receive the signals from the target user, and the TOA of the signals at different end sides of the LCX will be utilized as the indicator for filtering in the localization process. We establish a classic LCX channel model based on the geometrically based single-bounce (GBSB) model [19], which is based on the structure and bi-directional radiation characteristics of LCX, considering line-of-sight (LOS) signal condition and non-line-of-sight (NLOS) signal condition in an indoor space. Based on the model, we provide the numerical results of the localization performance by tracking a moving target user in the LCX communication system. The system measures the TOA of the user and then employs the particle filter for state estimation and localization using the TOA values. The TOA measurement of user signal is based on the multiple signal classification (MUSIC) algorithm.

II. LCX Structure and Radiation Property

A. LCX Radiation Property

Fig. 1(a) shows the LCX with a 4-layer structure used in this work. The periodic slots over the outer conductor can be equivalent to a uniform linear array of small magnetic dipole antennas. Radio waves can be radiated and received through these slots. When LCX is used as an antenna for wireless communication, the signal strength depends on the radio waves from all slots. Radiation angles with peak directivity of LCX can be expressed by

$$\theta_m = \sin^{-1}(\sqrt{\epsilon_r} + \frac{m\lambda}{P}), \qquad (m = -1, -2, \ldots) \quad (1)$$

where m is the harmonic order, P is the period of slots and ϵ_r is the LCX's relative insulator permittivity. λ is the wavelength related to the frequency band. m is set as -1 to avoid radiated harmonics. In addition, we can adjust the period P and the direction of slots to change the radiation angle of LCX.

Fig. 1(b) shows the anthor important property of LCX: bidirectional radiation property. The radiation direction will

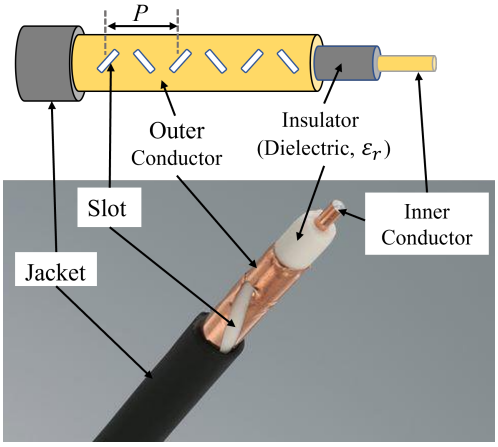

(a) The structure of leaky coaxial cable (LCX)

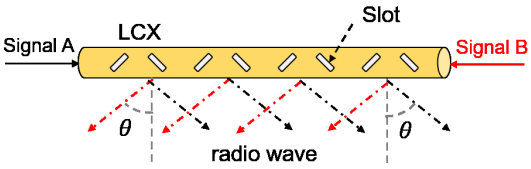

(b) Bidirectional radiation property of LCX

Fig. 1. The structure and radiation property of LCX.

appear an intersection angle of 2θ when signal A and signal B are fed to both sides of the LCX simultaneously. Due to the low correlation between the radiation characteristics, one LCX can be used as two antennas for wireless communication.

B. LCX Channel Model

Considering the LOS component and NLOS component of the signal propagation. We give a simple geometrically based single-bounce (GBSB) model [19], which uses the basic theory in the communication field, to establish a classic model for the wireless communication system using LCX. Here, a brief introduction to channel modeling is provided in this section. It should be noted that the following model introduction just provides the received signal model of one end of the LCX, and the received signal from the other end can be modeled in the same way.

The LCX signal noted as S_{LCX} is composed of LOS signal S_{LOS} and NLOS signal S_{NLOS}, which can be expressed as

$$S_{\mathrm{LCX}} = S_{\mathrm{LOS}} + S_{\mathrm{NLOS}}, \quad (2)$$

where, S_{NLOS} and S_{LOS} is stochastic and deterministic process respectively. Fig. 2(a) shows the LOS propagation paths which have two parts including the path from user (Tx) to slot O_i in the air and the path from slot O_i to cable end in the cable. The uniform power attenuation in the cable can be expressed as $\alpha_i = 10^{\frac{-\alpha P(i-1)}{40}}$. α is the longitudinal amplitude attenuation constant per meter in LCX. $P(i-1)/2$ is the cable length between cable end and slot O_i. Similarly, the phase variations in cable can be expressed as $\beta_i = k_r P(i-1)/2$.

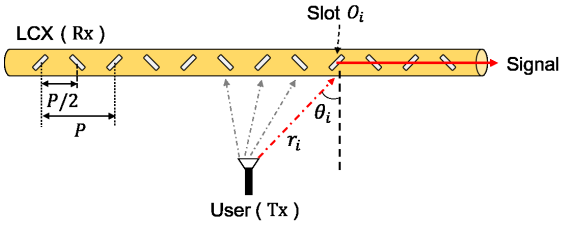

(a) LOS component

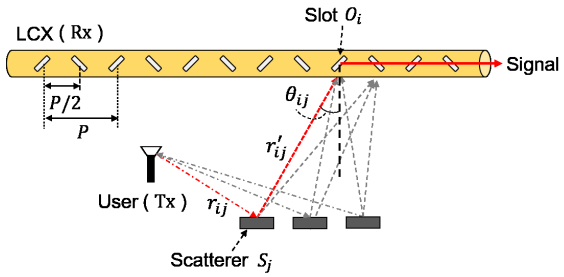

(b) NLOS component

Fig. 2. The LOS and NLOS propagation paths in LCX channel model.

k_r is the propagation constant of electrical waves in LCX and $k_r = k_0\sqrt{\epsilon_r}$. k_0 is the propagation constant in free space and $k_0 = 2\pi f/c$. c is the speed of light. Here, the values of k_r and k_0 can be changed by changing the value of f to simulate the generation of signals of different frequencies in free space and LCX. r_i is set as the distance from user Tx, which has one monopole antenna, to the center point of slot O_i. S_{LOS} depends on the superposition of LOS signals from all slots and can be expressed as

$$\begin{aligned} S_{\mathrm{LOS}} &= \sum_{i=1}^{N} S_{O_i} \\ &= \sum_{i=1}^{N} \alpha_i \sqrt{P_l(r_i)\cdot E(\theta_i)}\cdot e^{-j(k_0 r_i+\beta_i)}, \end{aligned} \tag{3}$$

where S_{O_i} is the signal from user Tx via slot O_i to the cable end. N is the number of slots. $E(\theta_i)$ is the power gain due to the radiation angle [15]. Function $P_l(r_i)$ represents the pathloss at a distance of r_i in indoor environment over 2.4 GHz band and can be expressed by

$$P_l(d) = 18.7\log_{10}d + 46.8 + 20\log_{10}(\frac{2.4}{5}), \tag{4}$$

where d is the distance of the propagation path.

Fig. 2(b) shows the NLOS component of the signal propagation. In the same way, we can express the NLOS signal S_{NLOS} simply as

$$\begin{aligned} S_{\mathrm{NLOS}} &= \sum_{i=1}^{N}\sum_{j=1}^{M} S_{O_{ij}} \\ &= \sum_{i=1}^{N}\sum_{j=1}^{M} \alpha_i \sqrt{P_l(r_{ij}+r'_{ij})\cdot E(\theta_{ij})}\cdot e^{j\varphi_{ij}} \\ &\cdot e^{-j(k_0(r_{ij}+r'_{ij})+\beta_i)}. \end{aligned} \tag{5}$$

Here, $S_{O_{ij}}$ means the signal from user Tx via scatterer S_j and slot O_i to cable end. r_{ij} and r'_{ij} represent the distance from Tx to scatterer S_j and the distance from scatterer S_j to slot O_i. φ_{ij} is the i.i.d random variables with uniform distributions at [0,2π).

C. TOA Measurement by MUSIC method

TOA as the timing information of the signal is often used in localization. The conventional localization method using LCX uses TDOA values and signal radiation angle to geometrically calculate the target location [16]. In this work, we use the MUSIC algorithm to measure TOA values as the indicator for particle filtering. The main idea of the TOA measurement using MUSIC is to estimate the noise subspace from available samples and search for steering vectors that are as orthogonal to the noise subspace as possible. The signal arrival can be estimated by searching the largest peak in the MUISC spectrum.

Here, we give a brief introduction on the TOA measurement using MUSIC algorithm. Given an $M \times M$ autocorrelation matrix from the signal samples at different frequency f as

$$\begin{aligned} \mathbf{Rx} &= \sum_{i=1}^{M} d_i \mathbf{V}_i \mathbf{V}_i^H \\ &= \sum_{i=1}^{s} (\lambda_i + \sigma_w^2)\mathbf{V}_i\mathbf{V}_i^H + \sum_{i=s+1}^{M} \sigma_w^2 \mathbf{V}_i\mathbf{V}_i^H, \end{aligned} \tag{6}$$

where the d_i and $\mathbf{V}_i$ are the eigenvalue and the eigenvector corresponding to the eigenvalue. The superscript H represents the Hermitian transpose. λ_i is the eigenvalue corresponding to the signal and σ_w^2 is the variance of white noise. M represents the number of equally spaced frequency points in one measurement. The eigenvectors corresponding to the s largest eigenvalues span the signal subspace. The remaining $M-s$ eigenvectors span the orthogonal noise space. We define the estimation function for MUSIC as

$$g(\tau) = \frac{1}{\sum_{i=s+1}^{M} \left|\mathbf{V}_i^H \mathbf{e}(\tau)\right|^2}, \tag{7}$$

where $\mathbf{e}(\tau)$ is known as the steering vector and can be expressed as

$$\mathbf{e}(\tau) = \left[1, e^{-j2\pi f_1\tau}, e^{-j2\pi f_2\tau}, \cdots, e^{-j2\pi f_M\tau}\right]^T, \tag{8}$$

$$\tau = nT_r, (n = 0, 1, 2, \cdots, N_s - 1). \tag{9}$$

T_r is the time resolution of MUSIC method. $f_1, f_2, ..., f_M$ are the equally spaced frequency points. N_s is the number of elements in pseudo spectrum. The orthogonality between the noise subspace and the steering vectors will minimize the denominator in Eq. (7) to 0 value. However, it is a small value in practice due to the noise. As a result, it will give rise to a peak, which corresponds to the signal arrival, in $g(\tau)$. From that, we can estimate the TOA of signals.

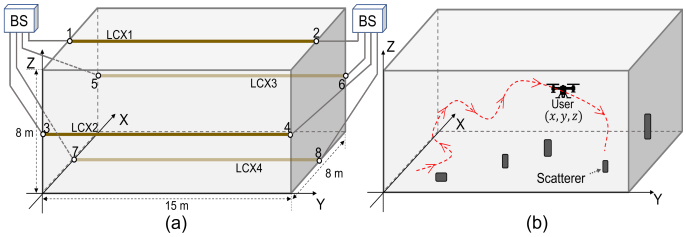

Fig. 3. System model in indoor environment. (a) LCX placement. (b) User motion and scatterers

III. Particle Filter-based Localization Method using LCX

As shown in Fig. 3, this paper considers the indoor environment as a three-dimensional (3-D) space with a length, width, and height of 15 m, 8 m, and 8 m. The user (which can be seen as a UAV device) with one monopole antenna moves in this space. It assumes that several scatterers are randomly distributed. Four LCXs are set to receive signals from the user. The cable ports are numbered from 1 to 8. Signal processing and particle filtering process will be done by the base stations (BS) at both ends of the LCX.

A. Motion State Model

The motion state model is built in a 3-D cartesian coordinate. We set a vector U_t to represent the motion state of the user at time t. U_t can be written as $[x_t, y_t, z_t, \theta_t, \varphi_t, l_t]^{\mathrm{T}}$, where (x_t, y_t, z_t) defines the 3-D location of the user. θ_t and φ_t are the elevation angle and azimuth of the moving orientation. l_t is the stride length. The state transition can be described by the following equation as

$$U_t = \begin{pmatrix} 1 & 0 & 0 & 0 & 0 & cos(\varphi_{t-1}) \cdot cos(\theta_{t-1}) \\ 0 & 1 & 0 & 0 & 0 & cos(\varphi_{t-1}) \cdot sin(\theta_{t-1}) \\ 0 & 0 & 1 & 0 & 0 & sin(\varphi_{t-1}) \\ 0 & 0 & 0 & 1 & 0 & 0 \\ 0 & 0 & 0 & 0 & 1 & 0 \\ 0 & 0 & 0 & 0 & 0 & 1 \end{pmatrix} U_{t-1} + [0 \;\; 0 \;\; 0 \;\; \Delta\theta \;\; \Delta\varphi \;\; \Delta l]^{\mathrm{T}} + n_{t-1}, \tag{10}$$

where U_{t-1} is the motion state at time $t-1$. n_{t-1} represents the process noise in state transition at time $t-1$. $\Delta\theta$, $\Delta\varphi$ and Δl represent the variations of the moving orientation and stride length at the end of each time step. The values of $\Delta\theta$, $\Delta\varphi$ and Δl vary randomly within a specified range, so the user performs non-linear motion in this model. We set state transition as function $F(\cdot)$.

The signal received at the LCX side from the user is simulated using the LCX channel model in Section II. We measure the TOA of the LCX received signal at each cable end using the MUSIC method. The observation frequency band is set on the 2.4 GHz band with a bandwidth of 76.25 MHz and the frequency interval is set as 312.5 KHz which is the same as the subcarrier in IEEE802.11n/ac. We define the TOA of the signal from port 1 to port 8 in Fig. 3(a) as $t_1, t_2, ..., t_8$. The TOA measurement value of target user at time t is M_t, which can be expressed as $[t_1, t_2, ..., t_8]$.

B. Particle Filtering

Particle filtering algorithm is based on recursive Bayesian and Monte Carlo simulation [8]. The key idea of a particle filter is using discrete random samples (particles) instead of the conventional integral calculation. Particles are used to approximate the probability density function of the nonlinear system to achieve the minimum variance estimation of the system state. Indoor localization can also be seen as a kind of filtering process, and we can use the particle filter algorithm to solve estimation problems. The main idea is to determine the posterior probability distribution of the system using noisy observations. The posterior probability distribution consists of particles with weights.

Algorithm 1: Particle Filter-based localization

Data: M_t, T, N_p
Result: User localtion
Initialize the weight and location distribution of particles ;
for $t = 2, 3, ..., T$ **do**
  ***Step 1*: Sampling and Calculating Weights** ;
  for $i = 1 : N_p$ **do**
    Update the particle states: $P_t^i = F(P_{t-1}^i) + \xi$;
    Obtain the particle TOA vector $M_{p_t}^i$ using LCX chennel model and MUSIC method ;
    Calculate the particle weights: $w_t^i = \frac{1}{\sqrt{(2\pi)^{\varepsilon}|\Sigma|}} e^{-\frac{\left(M_t - M_{p_t}^i\right)^{\mathrm{T}} \Sigma^{-1} \left(M_t - M_{p_t}^i\right)}{2}}$;
  end
  ***Step 2*: Normalization of Particle Weights** ;
  $w_{sum} = \sum_{i=1}^{N_p} w_t^i$;
  for $i = 1 : N_p$ **do**
    $w_t^i = \frac{w_t^i}{w_{sum}}$;
  end
  ***Step 3*: Particle Resampling** ;
  Resmaple the particles (Algorithm 2) ;
  ***Step 4*: Location Estimation** ;
  Calculate the estimated location of user: $(x_t, y_t, z_t) = \sum_{i=1}^{N_p} w_t^i \cdot P_t^i$;
end

In this work, we define the particle state at time t as P_t^i and the update of the particle can be expressed by:

$$P_t^i = F(P_{t-1}^i) + \xi, \tag{11}$$

$$P_t^i = [x_{p_t}^i, y_{p_t}^i, z_{p_t}^i, \theta_{p_t}^i, \varphi_{p_t}^i, l_{p_t}^i]^{\mathrm{T}}, i = 1, 2, ..., N_p, \tag{12}$$

where $F(\cdot)$ is the state transition mentioned above, and N_p is the number of particles. ξ is thw zero-mean Gaussian random noise. $(x_{p_t}^i, y_{p_t}^i, z_{p_t}^i)$ is the 3-D location of i-th particle at time t. The TOA indicator of the particle can be expressed as $M_{p_t}^i$ which can be obtained using the LCX channel model

and MUSIC algorithm in previous section. The posterior probability of user state U_t can be approximated as

$$p(U_t|M_{1:t}) \approx \sum_{i=1}^{N_p} w_t^i \delta(U_t - P_t^i), \tag{13}$$

where $\delta(\cdot)$ is the Dirac delta function. w_t^i is the weight of particle P_t^i and can be obtained by

$$w_t^i = \frac{1}{\sqrt{(2\pi)^{\varepsilon}|\Sigma|}} e^{-\frac{\left(M_t - M_{p_t}^i\right)^{\mathrm{T}} \Sigma^{-1} \left(M_t - M_{p_t}^i\right)}{2}}, \tag{14}$$

where Σ is the covariance matrix of measurement noise.

In particle filter, the number of effective particles N_{eff} is usually used to observe the degree of depletion of particle weights. N_{eff} can be defined as

$$N_{eff} \approx \frac{1}{\sum_{i=1}^{N_p} (w_t^i)^2}. \tag{15}$$

When the value of N_{eff} becomes small, the variance of the weights becomes large which indicating that the depletion of particle weights. In this paper, we choose the Random Resampling Algorithm for particle resampling in the filtering process. After particle resampling, the estimated location of the user can be calculated using the weighted particles.

Algorithm 2: Random Resampling Algorithm

Data: w_t^i
Result: n_t^i(particle number)
Generate u containing N_p random numbers from the continuous uniform distributions on the interval $(0, N_p)$;
Sort the numbers in u in ascending order ;
Calculate the cumulative sum of weights: $C_i = Accumulate(w_t^i)$;
$j = 1$;
for $k = 1 : N_p$ **do**
  while $(j \leq N_p)$ & $(u_j \leq C_k)$ **do**
    $n_i = k$;
    $j = j + 1$;
  end
end

IV. Performance Evaluation

We use the distance between the user's real location and the estimated location as the localization error to investigate the performance of the proposal. The target user will move in the space for several times, and then the localization errors are counted. In addition, we also investigate the effect of the number of particles used and the number of LCXs on the localization performance. The specifications of the LCX and other detailed parameters and conditions in the simulation are listed in Table I.

Fig. 4 is the localization error results using different numbers of particles. The mean value of the location error, when the number of particles N_p is set as 1000, is 0.94 m. When N_p is set as 100 and 500, the location errors are 2.47 m and 1.43 m respectively. As the results show, the performance of the proposed localization method using particle filter is promising. As the number of particles used in the process decreases, the localization performance of the proposed method drops severely.

TABLE I
Simulation Specifications

Parameter	Value
LCX type	LCX1, LCX2 (V1-type) LCX3, LCX4 (V2-type)
LCX slot period [m]	0.04 (V1), 0.03 (V2)
Maximum radiation angle [deg]	18 (V1), 55 (V2)
Shortening coefficient in LCX	0.6403 (for all)
Cable loss [dB/m]	0.6 (for all)
Frequency bandwidth [MHz]	76.25 (2403.9-2480.15)
Frequency interval [KHz]	312.5
Number of scatterers (M)	50
Number of particles (N_p)	100, 500, 1000
Number of LCXs (N_{LCX})	Pattern A: 2 (LCX1, LCX2) Pattern B: 3 (LCX1, LCX2, LCX3) Pattern C: 4 (all LCXs)
Time step size (T)	20

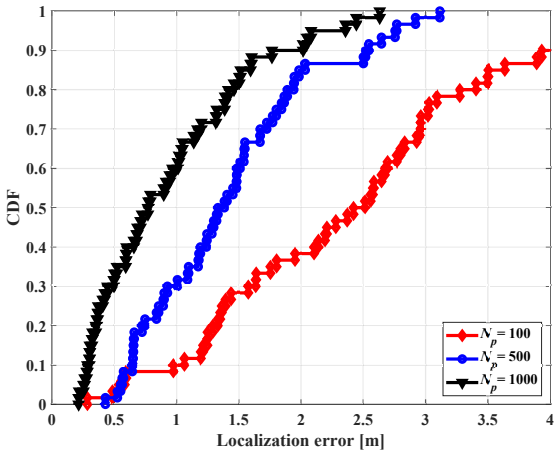

Fig. 4. Localization errors when using a different number of particles. (Pattern C, $N_{\mathrm{LCX}} = 4$)

Fig. 5 shows the localization error results when using different numbers of LCXs. The number of the particles N_p is set as 1000. We consider the LCX placement as three patterns from Pattern A to Pattern C using 2, 3, and 4 LCXs respectively. In the order of increasing the number of LCXs used, the mean localization errors are 2.62 m, 1.36 m, and 0.94 m. From the results, we can find that the localization performance of the proposal gets better when using more LCXs in the localization system.

Fig. 6 is the comparison of the localization errors with a different number of scatterers. When the number of scatterers M is 0, which means no NLOS propagation in the communication environment, the average localization error is 0.62 m with a 90% accuracy of 1.1 m. As the number of scattering points increases, the localization performance gets

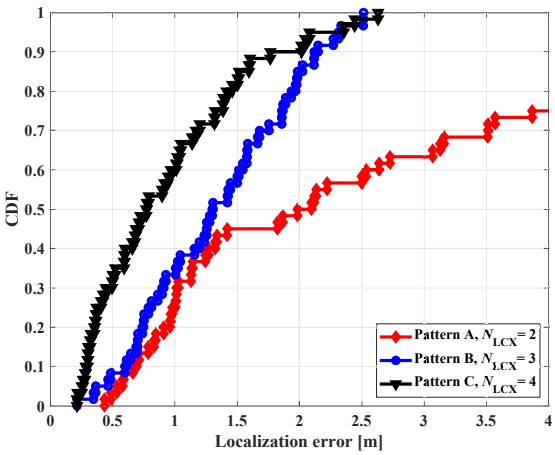

Fig. 5. Localization errors with a different number of LCXs. ($N_p = 1000$)

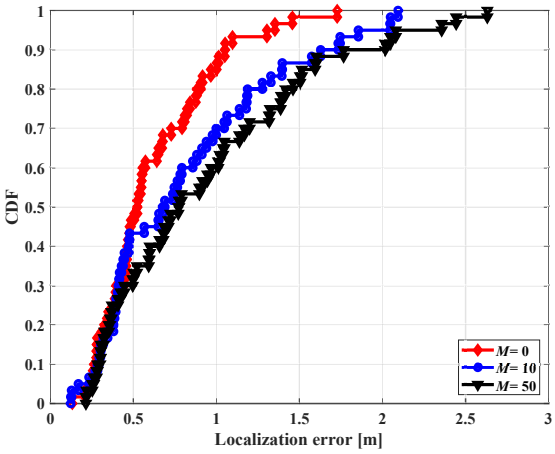

Fig. 6. Comparison of the localization errors with a different number of scatterers in the simulation model. (Pattern C, $N_{\mathrm{LCX}} = 4$, $P_n = 1000$)

worse due to the impact of the NLOS problem. However, the increase in the number of scattering points does not greatly degrade the localization performance. This result shows that the TOA-based LCX localization method using the particle filtering algorithm can perform well in a multipath-rich indoor environment.

V. Conclusion

This paper proposed a particle filter-based 3-D localization method using LCX in an indoor environment. The proposed method measures the TOA value of the signal from the user terminal as the indicator and performs particle filtering to estimate the user location. The results of the localization errors show that the particle filter-based method is promising and can provide a good localization performance in a multipath-rich indoor environment.

Acknowledgement

This work was supported by the JSPS KAKENHI Grand Number 20K04484, JST SPRING Grand Number JPMJSP2126, and the GMO Internet Foundation.

References

[1] S. Kuutti, S. Fallah, K. Katsaros, M. Dianati, F. Mccullough and A. Mouzakitis, "A survey of the state-of-the-art localization techniques and their potentials for autonomous vehicle applications," *IEEE Internet of Things Journal*, vol. 5, no. 2, pp. 829-846, Mar. 2018.

[2] F. Zafari, I. Papapanagiotou, and K. Christidis, "Microlocation for Internet-of-Things-Equipped Smart Buildings," *IEEE Internet of Things Journal*, vol. 3, no. 1, pp. 96–112, 2016.

[3] A. Al-Fuqaha, M. Guizani, M. Mohammadi, M. Aledhari and M. Ayyash, "Internet of Things: A Survey on Enabling Technologies, Protocols, and Applications," *IEEE Communications Surveys & Tutorials*, vol. 17, no. 4, pp. 2347-2376, fourthquarter 2015.

[4] W. Kwon, J. H. Park, M. Lee, J. Her, S. -H. Kim and J. -W. Seo, "Robust autonomous navigation of unmanned aerial vehicles (UAVs) for warehouses' inventory application," *IEEE Robotics and Automation Letters*, vol. 5, no. 1, pp. 243-249, Jan. 2020

[5] W. Miao, C. Luo, G. Min, Y. Mi and Z. Yu, "Location-based robust beamforming design for cellular-enabled UAV communications," *IEEE Internet of Things Journal*, vol. 8, no. 12, pp. 9934-9944, 15 June15, 2021

[6] X. Wang, L. Gao, S. Mao and S. Pandey, "CSI-Based Fingerprinting for Indoor Localization: A Deep Learning Approach," *IEEE Transactions on Vehicular Technology*, vol. 66, no. 1, pp. 763-776, Jan. 2017.

[7] C. Hsieh, J. Chen and B. Nien, "Deep Learning-Based Indoor Localization Using Received Signal Strength and Channel State Information," *IEEE Access*, vol. 7, pp. 33256-33267, 2019.

[8] P. M. Djuric, J. H. Kotecha, J. Zhang, Y. Huang, T. Ghirmai, M. F. Bugallo, and J. Miguez, "Particle filtering," *IEEE Signal Processing Magazine*, vol. 20, no. 5, pp. 19–38, Sep. 2003.

[9] J. L. Carrera Villacrés, Z. Zhao, T. Braun and Z. Li, "A Particle Filter-Based Reinforcement Learning Approach for Reliable Wireless Indoor Positioning," *IEEE Journal on Selected Areas in Communications*, vol. 37, no. 11, pp. 2457-2473, Nov. 2019.

[10] J. W. Huang, K. K. Mei, "Theory and analysis of leaky coaxial cables with periodic slots," *IEEE Transactions on Antennas and Propagation*, vol. 49, no. 12, pp. 1723–1732, Dec. 2001.

[11] J. H. Wang, "Research on the radiation characteristics of patched leaky coaxial cable by FDTD method and mode expansion method," *IEEE Transactions on Vehicular Technology*, vol. 57, no. 1, pp. 90–96, Jan. 2008.

[12] D. Dudley, M. Lienard, S. Mahmoud and P. Degauque, "Wireless propagation in tunnels," *IEEE Antennas and Propagation Magazine*, vol. 49, no. 2, pp. 11–26, Apr. 2007.

[13] T. Okamoto, Q. T. Duong, T. Higashino and M. Okada, "A proposal of data transmission in parallel line fed wireless power transfer," *2015 15th International Symposium on Communications and Information Technologies (ISCIT)*, pp. 85-88, 2015.

[14] Y. Hou, S. Tsukamoto, S. Li, T. Higashino, K. Kobayashi and M. Okada, "Capacity evaluation of MIMO channel with one leaky coaxial cable used as two antennas over linear-cell environments," *IEEE Trans. on Vehicular Technology*, vol.66, no.6, pp. 4636–4646, June 2017.

[15] Y. Hou, J. Zhu, S. Denno and M. Okada, "Capacity of 4-by-4 MIMO channel using one composite leaky coaxial cable with user position information," *IEEE Transactions on Vehicular Technology*, vol. 68, no. 11, pp. 11042-11051, Nov. 2019.

[16] K. Nishikawa, T. Higashino, K. Tsukamoto and S. Komaki, "A new position detection method using leaky coaxial cable," *IEICE Electronics Express*, vol. 5, no. 8, pp. 285–290, Aug. 2008.

[17] S. Oki, Y. Hou, T. Higashino, M. Okada, "Two-dimensional positioning for radio terminal in 4-by-4 MIMO system using leaky coaxial cable antenna," *ITE Technique Report*, vol. 39, no. 4, pp. 45–48, Jan. 2015.

[18] J. Zhu, P. Hou, K. Nagayama, Y. Hou, S. Denno and R. Ferdian, "Two-dimensional RSSI-based indoor localization using multiple leaky coaxial cables with a probabilistic neural network," *Access*, vol. 10, pp. 21109-21119, 2022

[19] K. Zhang, F. Zhang, G. Zheng, A. Saleem, "GBSB model for MIMO channel using leaky coaxial cables in tunnel," *IEEE Access*, vol. 7, pp. 67646 - 67655, May. 2019

[20] M. Zhang, T. Qing, J. Zhu and W. Shen, "Indoor positioning tracking with magnetic field and improved particle filter," *International Journal of Distributed Sensor Networks*, vol. 13, no. 11, pp. 1550147717741835